Appl Phys B (2012) 106:393–398
DOI 10.1007/s00340-011-4723-9

Applied Physics B
Lasers and Optics

Achromatic terahertz quarter-wave retarder in reflection mode

L. Sun · Z. Lü · D. Zhang · Z. Zhao · J. Yuan

Received: 28 April 2011 / Revised version: 2 July 2011 / Published online: 11 September 2011

Abstract A compact achromatic quarter-wave retarder (QWR) operating in reflection mode is designed for using in terahertz region. It is a composite device utilizing form birefringence and Fabry–Pérot (FP) interference. Under illumination of plane waves with incidence angle of 45°, from 1.8 THz to 2.8 THz, the QWR achieved only ±2° variation around 90° phase retardation, enlarging the working bandwidth of ordinary QWR greatly. An analytical model combining transmission-line (TL) theory with effective medium theory (EMT) is presented and results agree well with the time-consuming numerical calculation. The 38 μm thick construction is simple and easy for fabrication by the existing lithographic technique and a promising application in terahertz or other frequency region is believed.

1 Introduction

Terahertz, as a newly exploited electromagnetic (EM) wave, promises a bright future in a wide spread of application areas. It has potential uses for spectroscopic imaging, high bandwidth communication and sensitive detection for medical or biological issues [1, 2]. For these uses, various polarizing elements in this frequency range are demanding [3], including tunable and fixed phase shifters, filters, splitters, wave plates and so on. Among them, quarter-wave retarder(QWR) is one of the most fundamental ones, which introduces 90° phase shift between two orthogonally polarized electric components. Here, we focus our attention on the achromaticity of QWR, which is a often employed and investigated character of QWR.

Typical QWR using natural birefringent material is strongly dependant on wavelength. However, due to the dispersion of form birefringence [4], subwavelength gratings (SWG) are tailored to perform achromatic phase retardation, with a fill factor being about 0.7 to 0.8 [5, 6]. Another method for achromaticity is the use of total reflection, a kind of which is the well known Fresnel rhomb [4]. Combining SWG with total reflection, a reflective achromatic phase retardation is designed in both visible and near-infrared regions [7]. In addition, liquid crystal [8, 9] and multilayer bicrystalline materials [10] are also widely investigated for broadband operation. In fact, the most efficient and sophisticated QWR is in the nature. By experimental measurements and theoretical modeling, Roberts et al. discovered an excellent QWR in the eye of a stomatopod crustaceans, with ±2.7° variation in full visible range. This kind of achromaticity has proved to be the result of interplay between intrinsic and form birefringence in the eye [11]. More recently, anisotropic metamaterial with H-shaped periodic metallic pattern was designed successfully in manipulating polarization state of EM wave. Their theoretical calculation results showed that a wide band for phase retardation of 90° was achieved but the corresponding band for polarization conversion ratio of 0.5 was sharply narrow [12].

In terahertz region, methods used to produce QWR was various while discussion about achromaticity was limited. Dielectric SWGs have been fabricated for use at discrete frequencies [13, 14]. Birefringent negative-index metamaterial was creatively proposed to role as phase retarder. However, owing to the intrinsic resonant properties of metamaterial, the absorption of energy was severe and the working frequency band was narrow [15, 16]. Also, birefringence from electric resonance of metamaterial, as well as scaled

L. Sun (✉) · Z. Lü · D. Zhang · Z. Zhao · J. Yuan
Department of Physics, College of Science, National University of Defense Technology, Changsha, Hunan, 410073, P.R. China
e-mail: sunlin@nudt.edu.cn

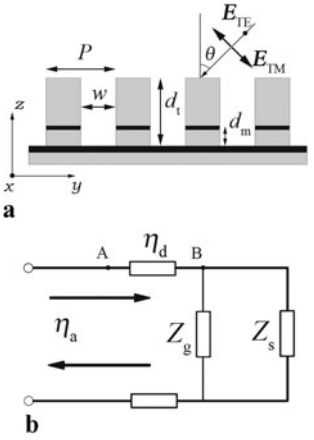

Fig. 1 The schematic of cross section of QWR (**a**) and the representation of equivalent TL model (**b**). In (**a**), the *gray section* represents dielectric medium while the *dark section* represents metal

double-layer meanderline structure, were used to fabricate terahertz quarter-wave plate working in narrow bandwidth [3, 17]. Combining up six quartz plates together, a quarter-wave plate operating from 0.25 to 1.75 THz was designed and fabricated [18]. However, with the bulk thickness of 31.4 mm, the device was not suitable for use in compact space. In study of generation of elliptically polarized terahertz pulses, Amer proposed a rough "quarter-wave plate" by simply assembling a wire-grid polarizer with a metal mirror, whereas the achromaticity was not achieved [19].

Inspired by the idea of Amer mentioned above [19] and the dispersion property of form birefringence [5], in this letter, we propose a new method of producing an achromatic QWR. This QWR is supposed to work in terahertz region in reflection mode, which is assumed to be illuminated by plane waves with an incidence angle of 45°. Numerical simulation results show that phase retardation of 90° ± 2° in a large frequency bandwidth is obtained. An approximate analytical model is established also, resulting in a good agreement with the numerical one. Further investigation reveals that the FP interference is found to be responsible for the achromaticity, which is helpful for the design of the achromatic QWR in other frequency region.

2 Numerical simulation

Shown in Fig. 1(a) is the cross section of the composite QWR. The whole structure is supposed to be infinite and not varying along x-direction. Covered on the metal ground plane are a dielectric grating with a depth of d_m, a thin metal-strip grating and another layer of dielectric grating in sequence. The total depth of the three-layered grating is d_t, with period of P and width of $(P - w)$. The QWR is illuminated obliquely by plane waves with an incidence angle of θ. Since the incident plane is in the y–z plane, the incident wave could be divided simply into transverse electric (TE) mode and transverse magnetic (TM) mode. The polarization of TE wave is along x-direction while the polarization of TM wave is perpendicular to x-direction.

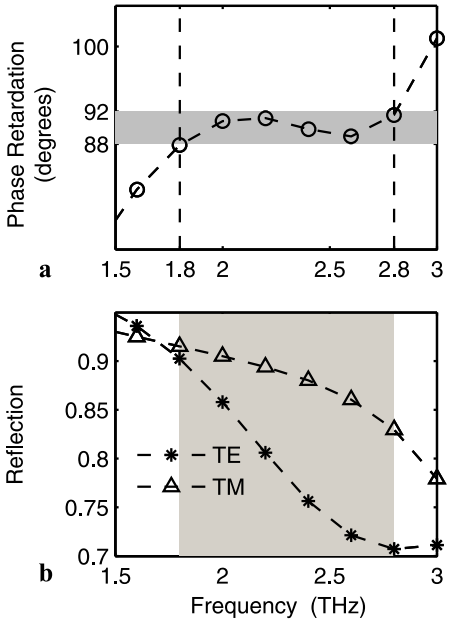

Fig. 2 Optimized performance of QWR by numerical calculation. The bandwidth with phase retardation between 88° and 92° is from 1.8 THz to 2.8 THz. The parameters are such that $P = 40$ μm, $w = 20$ μm, $d_t = 38$ μm, and $d_m = 15.8$ μm. Grey zone in (**a**) denotes the range of phase retardation from 88° to 92° while in (**b**) the range of frequency from 1.8 THz to 2.8 THz

Considering the feasibility of fabrication, we choose polyimide as the dielectric medium, with a refractive index of $1.8 - 0.04i$ in the terahertz region [20]. We select Au as the material of metal-strip grating whose thickness is fixed as 200 nm. Numerical calculation based on finite element method was carried out by a commercial software named COMSOL Multiphysics. In its RF module, we use in-plane scattered hybri-mode as field type. A rectangular domain including eight unite cells is calculated, with eight periods as the width and 600 μm as the length. Two boundaries along the propagation direction are set periodic and the anther two are set matched. By simulated annealing algorithm, an optimized QWR was obtained as shown in Fig. 2. The parameters are such that $P = 40$ μm, $w = 20$ μm, $d_t = 38$ μm, and $d_m = 15.8$ μm. Figure 2(a) exhibits phase retardation while Fig. 2(b) depicts reflectivities. Obviously, from 1.8 THz to 2.8 THz, about 1 THz of bandwidth for phase retardation of 90° ± 2° is achieved, which is nearly ten times of that achieved by the electric split ring resonator [17]. However, in the corresponding frequency range, the reflectivity of TE component is evidently unequal to that of TM component, which will reduce the degree of circular polarization. In our simulation, when the imaginary part of index of polyimide is set zero, the reflectivities of both TE and TM waves will turn to be unity. So, this kind of unequal reflectivities just results from the absorption of dielectric medium, which could be solved by choosing a material with lower or none absorption.

3 Analytical model

In order to verify the achromaticity obtained by numerical simulation, we established an analytical model based on transmission-line (TL) theory to calculate the reflection coefficients of TM and TE wave, respectively. As shown in Fig. 1(b), the equivalent TL model for QWR is depicted. For the grating period P being much smaller than the incident wavelength λ, it is reasonable to substitute the dielectric grating with an anisotropic homogeneous medium, whose permittivity could be obtained by effective medium theory (EMT) [21]. Considering the large imaginary part of permittivity of metal in terahertz region, metal components are approximated as perfect conductor with zero depth in our model. Following the dynamic modeling method introduced by Tretyakov et al. [22], the equivalent surface impedance could be easily found as the impedance of a parallel connection of the grid impedance Z_g and the input impedance Z_s of the grounded slab beneath the grids. The characteristic impedance along the TL is η_d in effective dielectric medium and η_a in air, respectively.

According to EMT, in effective dielectric medium, the permittivities are different for the fields parallel and perpendicular to the grating grooves. Here we have $\varepsilon_x = \varepsilon_z \neq \varepsilon_y$, where ε_i $(i = x, y, z)$ is the permittivity for the field along corresponding axis. Derived from the basic vector transmission-line equations, for plane waves, the boundary conditions of a planar dielectric slab on an ideally conducting surface could be written out exactly [23]. Then according to the definition of incidence impedance [24], the equivalent surface impedance at the surface of the grounded effective slab Z_s could be derived as for the TM wave:

$$Z_{s\_TM} = j\omega\mu\beta_{TM}\frac{\tan(\beta_{TM}d_m)}{k^2} \tag{1}$$

and for the TE wave:

$$Z_{s\_TE} = j\omega\mu\frac{\tan(\beta_{TE}d_m)}{\beta_{TE}} \tag{2}$$

where ω is the angular frequency, k denotes the wave number and μ is the permeability of effective dielectric medium. Notice that β_{TM} and β_{TE} are the propagation constant along z-axis for TM wave and TE wave, respectively, which could be written as [23]

$$\beta_{TM} = \sqrt{\frac{\varepsilon_y}{\varepsilon_z}\left(\omega^2\varepsilon_z\mu - {k_t}^2\right)}, \tag{3}$$

$$\beta_{TE} = \sqrt{\omega^2\varepsilon_x\mu - {k_t}^2} \tag{4}$$

Here, k_t is the tangential component of the wave number k. From the Snell equation [4], we could easily have $k_t = k_0\sin(\theta) = \sin(\theta)\sqrt{\omega^2\varepsilon_0\mu_0}$, in which k_0, ε_0 and μ_0 are the wave number in air, the permittivity of air and permeability of air, respectively.

Under the condition of $P \ll \lambda$, through averaging boundary condition, the averaged current density and the averaged x-component of total electrical field at the position of averaged grids could be connected by impedance operator [23]. Since the metal is perfectly conducting and the azimuth angle $\varphi = \pi/2$, the grid impedance for TE wave could be simplified as

$$Z_{g\_TE} = j\frac{\eta}{2}\alpha \tag{5}$$

where the wave impedance in dielectric medium for TE wave $\eta = \sqrt{\mu/\varepsilon_x}$. The grid parameter α could be given as [23]

$$\alpha = \frac{kP}{\pi}\left[\log\frac{2P}{\pi w} + \frac{\zeta(3)}{2}\left(\frac{kP}{2\pi}\right)^2 + \frac{3\zeta(5)}{8}\left(\frac{kP}{2\pi}\right)^4 + \cdots\right] \tag{6}$$

where $\zeta(x)$ is the Riemann zeta function. The higher-order terms must be included if the period P is not much smaller than λ. For a subwavelength grating, from distances larger than P, the scattering field could be ragarded as plane waves. However, when $d_m < P$, the influence of Floquet modes diffracted by metal-strip gratings could not be ignored. Treating the ground plane as a mirror for both incidence field and averaged current density, Wait found that the only influence of the evanescent modes to the reflection coefficient is the substitution $(\alpha + \gamma)$ instead of α [25].

For TM wave, the situation is a little complicated because the metal grid is imbedded in an anisotropic medium here. According to Šantavý's theorem about the Babinet principle used in electrically anisotropic medium [26], the field of TM wave could be transformed to its complementary filed of TE wave by transforming the coordinate system (assuming the mesh is along x-axis):

$$x = x', \quad y = \sqrt{\frac{\varepsilon_x}{\varepsilon_z}}y', \quad z = \sqrt{\frac{\varepsilon_x}{\varepsilon_y}}z' \tag{7}$$

where x, y, z are coordinates for TM wave and x', y', z' are coordinates for TE wave. Then, using the Babinet principle [24], the grid impedance for TM wave could be determined as

$$Z_{g\_TM} = \frac{\eta_{avg}^2}{4Z'_{g\_TE}} \tag{8}$$

where $\eta_{avg}^2 = \mu/\sqrt{\varepsilon_x\varepsilon_y}$ and the grid impedance for complementary TE wave Z'_{g_TE} could be obtained by solving (5), with the parameters P, w and k being adjusted accordingly.

Since now the loading impedance at point B is $Z_L = 1/(\frac{1}{Z_g} + \frac{1}{Z_s})$, from TL theory we obtain

$$Z_{in} = \eta_d \frac{Z_L + j\eta_d \tan(\beta l)}{\eta_d + jZ_L \tan(\beta l)} \tag{9}$$

as incidence impedance at point A, where the propagation length along the TL $l = d_t - d_m$, the propagation constant β could be obtained from (3) or (4), and the characteristic impedance of dielectric under oblique illumination η_d is [23]

$$\eta_{d\_TM} = \sqrt{\frac{\mu}{\varepsilon_y}} \sqrt{1 - \frac{k_t^2}{\omega^2 \varepsilon_z \mu}} \tag{10}$$

for TM wave and is

$$\eta_{d\_TE} = \sqrt{\frac{\mu}{\varepsilon_x}} \Big/ \sqrt{1 - \frac{k_t^2}{\omega^2 \varepsilon_x \mu}} \tag{11}$$

for TE wave. Finally, the reflection coefficient of a plane wave impinging obliquely on the structure could be written as

$$R = \frac{Z_{in} - \eta_a}{Z_{in} + \eta_a} \tag{12}$$

where η_a is the characteristic impedance in air and has the same form as η_d in (10) or (11).

4 Results and discussion

Using the analytical model descried above, we obtained the properties of QWR and compared them with the results calculated by numerical simulation. To avoid propagation of higher-order Floquet modes, the grating period P was chosen smaller than about 40 μm, by which the second-order effective indices obtained by EMT is qualitatively validated in the range concerned [27]. Making a tradeoff between the absorption and working bandwidth, the total depth d_t was chosen. Considering the facility of fabrication process, the geometrical parameters here are such that $P = 30$ μm, $d_t = 40$ μm, $f = 0.44$, and $f_d = 0.43$, where the fill factor f is defined as $f = (P - w)/P$ and the depth ratio f_d is as $f_d = d_m/d_t$. Shown in Fig. 3(a) and (c) are the results of both analytical and numerical calculation, with phase retardation in (a) and reflection in (c), respectively. Comparison between the results by two methods exhibits disagreement to some extent, where an obvious departure in high frequency region is observed. Investigation shows that there are mainly two points responsible for this in our analytical model. The first one is the use of EMT, which is just an approximate method even under the condition of long-wavelength limit. The second one is the effect of higher-order Floquet modes

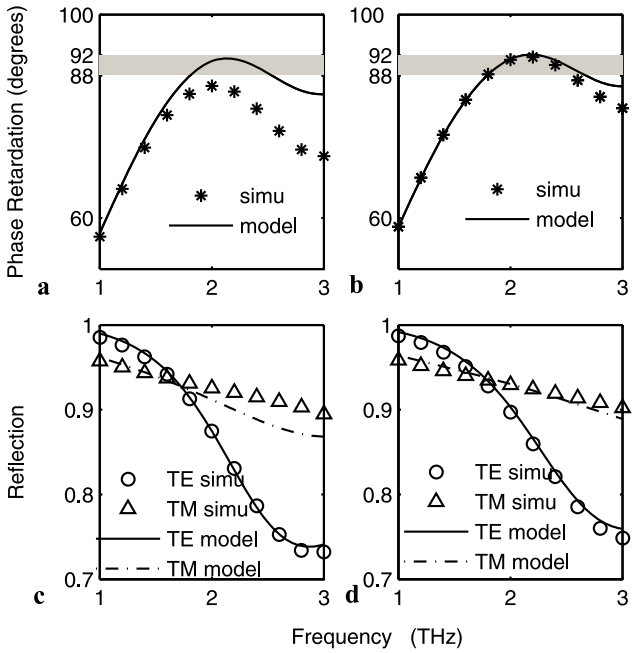

Fig. 3 Phase retardation and reflectivities of both analytical and numerical calculation. (**a**), (**b**) Display phase retardation while (**c**), (**d**) display reflectivities. *Circle-*, *triangle-* and *asterisk*-marks represent the results of numerical calculation while *solid line* and *dash-dotted line* represent the results of analytical calculation. Geometric parameters are as follows: $d_t = 40$ μm, $f = 0.44$, $f_d = 0.43$ and $P = 30$ μm for (**a**), (**c**) while $P = 10$ μm for (**b**), (**d**)

diffracted by subwavelength periodically arranged metal-strip grating. As we illustrated in the analytical model section above, when the metal-strip grating is close enough to the metal ground plane, the evanescent higher-order Floquet modes will be reflected back and forth between them. For TE wave, this effect could be solved by a mirrored method. However, for TM wave where the Barbinet's complementary principle is used, this effect could not be included in model because Barbinet's principle is just valid in situation of a single plane construction. Hence, the ignorance of higher-order Floquet modes for TM wave will introduce impreciseness to the model. This is verified by the results shown in Fig. 3(b) and (d), where only the period P is changed from 30 μm to 10 μm. In this case, the satisfied condition $d_m > P$ makes the Floquet-mode effect negligible while the condition $P \ll \lambda$ makes the EMT more accurate. So, good agreement between two results are achieved, shown as in Fig. 3(b) and (d). This validates both the numerical and analytical model.

In order to investigate the basic principle of achromaticity for QWR, we examined the phase change Δ_{TE} and Δ_{TM} occurring on the interface of reflection for TE and TM waves, respectively. As we all know, metal-strip grating with subwavelength period is almost transparent for TM wave and opaque for TE wave. Therefore, the QWR proposed here could be approximated as two grounded slab, one for TE wave and the other for TM, with different refractive index

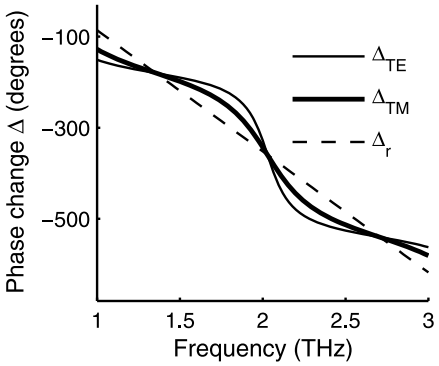

Fig. 4 Reflection phase change spectra from a grounded slab for both TE and TM waves, with $\varepsilon_r = 9$ and $h = 38$ μm. *Thin line* represents TE wave, *thick line* represents TM wave while *dashed line* represents the phase change of Δ_r

and different slab thickness. For simplicity, we started our investigation on a single grounded slab for both, with the same relative permittivity ε_r and the same thickness h. The incidence angle θ is assumed to be $\pi/4$. Using TL theory, we obtained the spectra of phase change Δ_TE and Δ_TM shown in Fig. 4. Obviously, both of them exhibit oscillation character with the same cycle. Moreover, we found that the balance line of those oscillating curves happens to be the phase change of the first order reflection Δ_r as the function of frequency, which is written as

$$\Delta_\mathrm{r} = \frac{4\pi}{\lambda_0}\sqrt{\varepsilon_r}h\cos\theta_\mathrm{t} + \pi \tag{13}$$

where λ_0 is the wavelength in free space, θ_t is the refraction angle. Hence, it is reasonable to attribute this kind of oscillation to the interference of multi-order reflections, which is also called the Fabry–Pérot interference [4]. To realize the achromaticity, we need to keep the phase retardation $\delta = \Delta_\mathrm{TE} - \Delta_\mathrm{TM}$ invariant over a certain frequency range, which means that the spectra of Δ_TE and Δ_TM should have different amplitudes but the same slope. If we only take into account the first order reflection, obviously from (13), the requirement for achromaticity will never be fulfilled. Thanks to the oscillation character induced by Fabry–Pérot interference, by choosing both proper ε_r and proper h for TE and TM wave, respectively, the requirement could be achieved thus the achromatic phase retarder could be realized. That is the basic principle of achromaticity of QWR proposed in this paper. However, it is not right to investigate the QWR just through the simple approximated grounded slab, since the subwavelength metal-strip grating for TE wave is not absolutely opaque. Take the corresponding SWG of optimized QWR in Fig. 2 for example, the transmission of TE wave at 2.8 THz is above 5%.

5 Conclusion

In summary, we proposed a new method of designing an achromatic QWR in terahertz region. The large working frequency bandwidth of the QWR was demonstrated by both numerical and analytical calculation. That is, from 1.8 THz to 2.8 THz, the phase retardation remains around 90° with variation of only ±2°. Further more, with the thickness of about 38 μm, this QWR has in its possession both the character of achromaticity and compactness, which may give it a promising application in various terahertz technologies. With the help of our analytical model and the basic working principle investigated, this QWR will be easy to design in other frequency region.

Acknowledgements This work is supported by the National Natural Science Foundation of China under Grant Nos. 10734140 and 60921062, the National Basic Research Program of China (973 Program) under Grant No. 2007CB815105. The authors also acknowledge the support of the College of Optoelectronic Science and Engineering, National University of Defense Technology (the New Century Excellent Talents in University of Ministry of Education of China under Grant No. 08-0142.)

References

1. M. Tonouchi, Nat. Photonics **1**, 97 (2007)
2. E. Pickwell, V.P. Wallance, J. Phys. D, Appl. Phys. **39**, 301 (2006)
3. X.G. Peralta, E.I. Smirnova, A.K. Azad, H.T. Chen, A.J. Taylor, I. Brener, J.F. O'Hara, Opt. Express **17**, 773 (2009)
4. M. Born, E. Wolf, *Principle of Optics* (Cambridge University Press, London, 1997)
5. H. Kikuta, Y. Ohira, K. Iwata, Appl. Opt. **36**, 1566 (1997)
6. G.P. Nordin, P.C. Deguzman, Opt. Express **5**, 163 (1999)
7. N. Passilly, K. Ventola, P. Karvinen, J. Turunen, J. Tervo, J. Opt. A, Pure Appl. Opt. **10**, 015001 (2008)
8. S. Shen, J. She, T. Tao, J. Opt. Soc. Am. **22**, 961 (2005)
9. R.P. Pan, C.W. Lai, C.J. Lin, C.F. Hsieh, C.L. Pan, Mol. Cryst. Liq. Cryst. **527**, 221 (2010)
10. S.S. Helen, M.P. Kothiyal, R.S. Sirohi, Opt. Commun. **154**, 249 (1998)
11. N.W. Roberts, T.H. Chiou, N.J. Marshall, T.W. Cronin, Nat. Photonics **3**, 641 (2009)
12. J. Hao, Y. Yuan, L. Ran, J.A. Kong, C.T. Chan, L. Zhou, Phys. Rev. Lett. **99**, 063908 (2007)
13. S.C. Saha, Y. Ma, J.P. Grant, A. Khalid, D.R.S. Cumming, Opt. Express **18**, 12168 (2010)
14. S.C. Saha, Y. Ma, J.P. Grant, A. Khalid, D.R.S. Cumming, IEEE Photonics Technol. Lett. **22**, 79 (2010)
15. C. Imhof, R. Zengerle, Opt. Commun. **280**, 213 (2007)
16. P. Weis, O. Paul, C. Imhof, R. Beigang, M. Rahm, Appl. Phys. Lett. **95**, 171104 (2009)
17. A.C. Strikwerda, K. Fan, H. Tao, D.V. Pilon, X. Zhang, R.D. Averitt, Opt. Express **17**, 136 (2008)
18. J.B. Masson, G. Gallot, Opt. Lett. **31**, 265 (2006)
19. N. Amer, W.C. Hurlbut, B.J. Norton, Y.S. Lee, T.B. Norris, Appl. Phys. Lett. **87**, 221111 (2005)
20. H. Tao, A.C. Strikwerda, K. Fan, C.M. Bingham, W.J. Padilla, X. Zhang, R.D. Averitt, J. Phys. D, Appl. Phys. **41**, 232004 (2008)
21. F. Träger, *Handbook of Lasers and Optics* (Springer, New York, 2007)

22. S.A. Tretyakov, C.R. Simovski, J. Electromagn. Waves Appl. **17**, 131 (2003)
23. S.A. Tretyakov, *Analytical Modeling in Applied Electromagnetics* (Artech House, Norwood, 2003)
24. J.A. Kong, *Electromagnetic Wave Theory* (Wiley, New York, 1986)
25. J.R. Wait, Can. J. Phys. **32**, 572 (1954)
26. I. Šantavý, Czechoslov. J. Phys. **17**, 216 (1967)
27. P. Lalanne, D.L. Lalanne, J. Mod. Opt. **43**, 2063 (1996)